

Phasons Formed on Si(100) Dimer Rows Observed by Scanning Tunneling Microscopy(STM-Si(100))

著者	Shigekawa Hidemi, Miyake Koji, Ishida Masahiko, Ozawa Satoshi, Hata Kenji
journal or publication title	Science reports of the Research Institutes, Tohoku University. Ser. A, Physics, chemistry and metallurgy
volume	44
number	1
page range	67-69
year	1997-03-28
URL	http://hdl.handle.net/10097/28680

Phasons Formed on Si(100) Dimer Rows Observed by Scanning Tunneling Microscopy

Hidemi Shigekawa, Koji Miyake, Masahiko Ishida, Satoshi Ozawa, and Kenji Hata

Institute of Materials Science, Center for Tsukuba Advanced Research Alliance (TARA),

University of Tsukuba, Tsukuba 305 Japan

(Received February 7, 1997)

At $\sim 6\text{K}$, dimers on Si(100) surface are buckled, and structural change occurs between $c(4\times 2)$ and $p(2\times 2)$ arrangements due to dimer flip-flop motion at phase boundaries on dimer rows. The phase defect appearing at boundaries has a structure similar to that of the type-C defect, two adjacent dimers are buckled in the same orientation. In consideration of the dimer arrangement around the phase boundary, there exist structures with two different conformations for the phase defect, however, according to the Ising spin model, both of which have the same energy higher compared to other buckled dimers with $2\times$ anticorrelation along a dimer row. Therefore, dimer flip-flop motion at a phase boundary results in the migration of a solitary phase defect with higher energy, as a phason.

KEYWORDS: STM, Si(100), dimer, $c(4\times 2)$, $p(2\times 2)$, defect, phason.

1. Introduction

It has widely been accepted that pairs of top-layer atoms form buckled dimers on the Si(100) surface¹⁾. Recently, an atomically resolved structural change between $c(4\times 2)$ and $p(2\times 2)$ arrangements of the Si(100) surface was observed at $\sim 6\text{K}$ by scanning tunneling microscopy (STM)²⁾. The observed change was due to the migration of phase defects of a new type on dimer rows, type-P defect, which have a structure similar to that of the type-C defect. Since a type-P defect consists of two adjacent dimers which are buckled in the same orientation, it works as a phase shifter. Therefore, dimer flip-flop motion at a phase boundary results in the migration of a solitary phase defect, like a phason. In this paper, we discuss the structure of the phase defect using the Ising spin model.³⁾

2. Experimental

Experiments were performed using a low-temperature STM that allowed observation with atomic resolution at $\sim 6\text{K}$ in ultrahigh vacuum ($5\times 10^{-9}\text{Pa}$). A phosphorus-doped ($0.005\ \Omega\cdot\text{cm}$) Si(100) sample surface was used.

3. Results and discussion

Figure 1 shows an STM image acquired continuously at $\sim 6\text{K}$. The surface was scanned in the constant current mode. The sample voltage V_s and tunneling current I_t were set at $+1.5\text{V}$ and 1.5nA , respectively. Each area in the images shows the change during scans of about four minutes. Areas with $c(4\times 2)$ or $p(2\times 2)$ arrangements coexist. At the phase boundaries on dimer rows, there exist some type-P defects as indicated by arrows in Fig. 1. In comparison of the two images, it is clear that the phase defects have moved during the scans.

First, let's see what kind of structural changes on the surface can be caused by the movement of a phase defect. Figure 2 shows three types of structural changes, (1) left side; $c(4\times 2) \rightarrow p(2\times 2)$, (2) central; at the dimer row on a domain boundary between $c(4\times 2)$ and $p(2\times 2)$

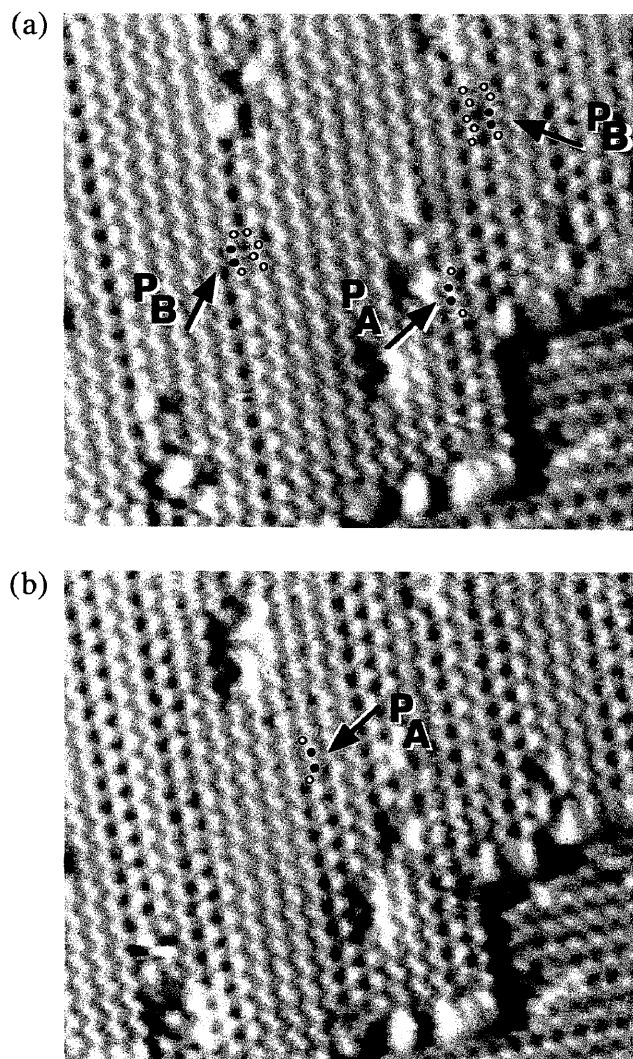


Fig. 1. STM images of Si(100) surface obtained continuously at $\sim 6\text{K}$ ($V_s=1.5\text{V}$, $I_s=1.5\text{nA}$). Each area in the images shows the change during scans of about four minutes. Two phases of $c(4\times 2)$ and $p(2\times 2)$ arrangements coexist. A and B indicate phase defects with two different conformations.

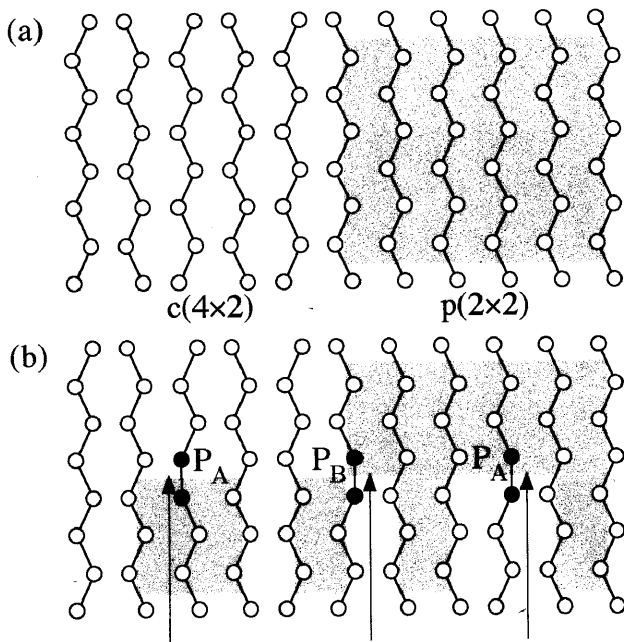


Fig. 2. (a) schematics of the boundary between $c(4 \times 2)$ and $p(2 \times 2)$ arrangements. (b) structural change caused by the introduction of a phase defect in each area in (a).

arrangement, and (3) right side; $p(2 \times 2) \rightarrow c(4 \times 2)$. Only the upper Si atoms of the buckled dimers are illustrated using circles. Lines between the circles are drawn in order to compare the phase shift. Phase defects are indicated by solid circles, and $p(2 \times 2)$ arrangement areas are dotted. Considering the conformations around the phase defects, they are classified into two categories; (A) phase defect in $c(4 \times 2)$ or $p(2 \times 2)$ arrangement ((1) and (3)), and (B) phase defect on a boundary ((2)). In the former, movement of a phase defect results in a structural change between $c(4 \times 2)$ and $p(2 \times 2)$ arrangements. On the other hand, in the latter case, the ratio between the amounts of the two arrangement areas does not change even if the phase defect migrates along the dimer row. These phase defects with the two different conformations were observed on the surface as indicated by A and B in Fig. 1. Figure 3 shows the magnified STM images of the two structures.

In order to consider the structures in Fig. 3, surface dimer structures are drawn by the schematics of the Ising spin model in Fig. 4: (a) $c(4 \times 2)$, (b) $p(2 \times 2)$, (c) a

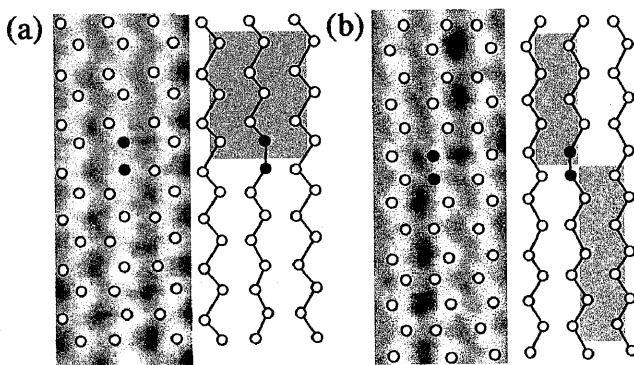


Fig.3. Magnified STM images of the two phase defects, structures of which correspond to those indicated by A and B in Fig. 1.

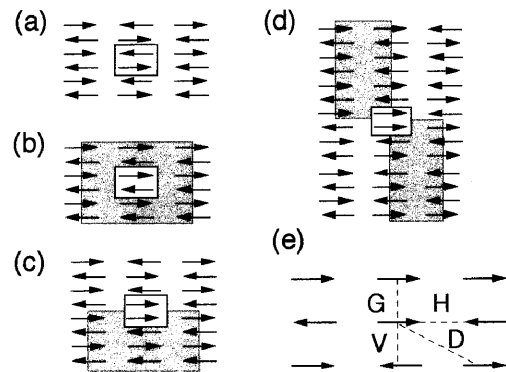


Fig. 4 Schematics of dimer structures: (a) $c(4 \times 2)$, (b) $p(2 \times 2)$, (c) a single type-P defect in $c(4 \times 2)/p(2 \times 2)$, (d) a single type-P defect on a dimer row at the boundary between areas with $c(4 \times 2)$ and $p(2 \times 2)$ arrangements, (e) coupling constants for the Ising model. Areas with the $p(2 \times 2)$ arrangement are colored gray. Type-P defects and similar units in the $c(4 \times 2)/p(2 \times 2)$ structures are indicated by rectangles for comparison.

single type-P defect in $c(4 \times 2)$ or $p(2 \times 2)$ arrangement, (d) a single type-P defect on a dimer row at the boundary between areas with $c(4 \times 2)$ and $p(2 \times 2)$ arrangements, (e) coupling constants for the Ising model. Areas with the $p(2 \times 2)$ arrangement are dotted. Type-P defects and similar units in the $c(4 \times 2)/p(2 \times 2)$ structures are indicated by rectangles for comparison. In the Ising spin model, it is assumed that the two degrees of freedom of an Ising spin correspond to the two possible orientations of an asymmetric Si-Si dimer. Absolute values of the coupling constants between Ising spins determined by Nakayama et al. shown in (e) are $V=51.9$ meV, $H=6.6$ meV, $D=3.6$ meV and $G=40$ meV³⁾.

Interaction energies of the two dimer units in the $c(4 \times 2)$ and $p(2 \times 2)$ area (Figs. 4(a) and (b)) are $-3V+4H-8D$ and $-3V-4H+8D$, respectively. Although the conformations of the phase defect units in Figs. 4(c) and 4(d) look different from each other, they have the same interaction energy of $-2V+G$. When the values indicated above are substituted, the energy in the solitary area becomes $90 \sim 95$ meV higher compared to the other buckled dimers with $2 \times$ anticorrelation along the dimer rows. The observed migration of type-P defects corresponds to the fluctuation of isolated higher-energy phase defect regions. Since the phase defects seem to move around easily even at ~ 6 K²⁾, energy barrier height for the dimer flip-flop motion must not be so high as previously predicted⁴⁾.

At room temperature, symmetric dimers are considered to consist of buckled dimers which flip-flop quickly. Taking into account the results of photoemission spectroscopy and LEED measurements, they mostly keep the anticorrelation along dimer rows even at room temperature^{5,6)}. In any case, $c(4 \times 2)$ and $p(2 \times 2)$ arrangements coexist at higher temperature region. On the other hand, as Wolkow et al. showed, $c(4 \times 2)$ arrangement is mostly formed on the surface around 100 K⁷⁻⁹⁾. However, $p(2 \times 2)$ arrangement area appears again at ~ 6 K²⁾. Therefore, when the temperature is decreased, the observed phase transition is (1) $c(4 \times 2) + p(2 \times 2) \rightarrow$ (2) $c(4 \times 2) \rightarrow$ (3) $c(4 \times 2) + p(2 \times 2)$. This surface structural change on the surface suggests a possibility that the coupling constants between

dimers are temperature dependent. Since the interaction energies of a dimer in $c(4 \times 2)$ and $p(2 \times 2)$ arrangements are $-2V+2H-4D$, and $-2V-2H+4D$, respectively, change in the ratio of H/D is most effective. If the interaction between the dimers depends on temperature, dynamics of the phase defect may change, however, essential idea about the structure of the phase defect formed on a dimer row is expected to remain. In any case, the energy difference between $c(4 \times 2)$ and $p(2 \times 2)$ arrangements is very small¹⁰⁾, theoretical calculation including temperature dependence is necessary to understand the surface structures. In a drastic case, energy balance between $c(4 \times 2)$ and $p(2 \times 2)$ arrangements may change.

Detailed analysis about the dynamics of the phase defect and related structural changes on the surface is in progress, which will be published elsewhere.

4. Conclusion

At $\sim 6K$, dimer flip-flop motion at phase boundaries on dimer rows was observed directly. The phase defect formed at boundaries has a structure similar to that of the type-C defect. Two type structures with two different conformations for the phase defect exist. However, according to the Ising spin model, both of them have the same energy higher compared to other buckled dimers with $2 \times$ anticorrelation along a dimer row. Therefore, dimer flip-flop motion at a phase boundary results in the migration of a solitary phase defect with higher energy like a phason.

Acknowledgements

This work was supported by Shigekawa Project of TARA, University of Tsukuba. Grant-in-Aid for Scientific Research from the Ministry of Education, Science and Culture of Japan is also acknowledged. One of the authors (K.M.) was financially supported by the Japan Society for the Promotion of Science (JSPS) Fellowships for Japanese Junior Scientists.

- 1) R. J. Hamers, R. M. Tromp, and J. E. Demuth, *Phys. Rev.* **B34** (1986) 5343.
- 2) H. Shigekawa, K. Miyake, M. Ishida, K. Hata, H. Oigawa, Y. Nannichi, R. Yoshizaki, A. Kawazu, T. Abe, T. Ozawa, and T. Nagamura, *Jpn. J. Appl. Phys.* **35** (1996) L1081.
- 3) Y. Nakamura, H. Kawai, and M. Nakayama, *Phys. Rev.* **B52** (1995) 8231.
- 4) A. Shkrebtii, R. D. Felice, M. Bertoni, and R. Del Sole, *Phys. Rev.* **B51** (1995) 11201.
- 5) T. Tabata, T. Aruga, and Y. Murata, *Surf. Sci.* **179** (1987) L63.
- 6) J. E. Northrup, *Phys. Rev.* **B47** (1993) 10032.
- 7) R. Wolkow, *Phys. Rev. Lett.* **68** (1992) 2636.
- 8) H. Tochiyama, T. Amakusa, and M. Iwatsuki, *Phys. Rev.* **B50** (1994) 12262.
- 9) A. R. Smith, F. K. Men, K. -J. Chao, and C. K. Shih, *J. Vac. Sci. Technol.* **B14** (1996) 914.
- 10) A. Ramstad, G. Brocks, and P. J. Kelly, *Phys. Rev.* **B51** (1995) 14505.